

# Chiral Symmetry Breaking and Pion Decay in a Magnetic Field

Prabal Adhikari<sup>1,2,\*</sup> and Brian C. Tiburzi<sup>3,4,†</sup>

<sup>1</sup>*Physics Department, Faculty of Natural Sciences and Mathematics, St. Olaf College, Northfield, MN 55057, USA*

<sup>2</sup>*Kawli Institute for Theoretical Physics, University of California, Santa Barbara, CA 93106, USA*

<sup>3</sup>*Department of Physics, The City College of New York, New York, NY 10031, USA*

<sup>4</sup>*Graduate School and University Center, The City University of New York, New York, NY 10016, USA*

The pattern of chiral symmetry breaking is exploited to compute vector and axial-vector pion matrix elements in a uniform magnetic field. Our results are model independent, and thereby constitute low-energy theorems that must be obeyed by QCD in external magnetic fields. Chiral perturbation theory and lattice QCD results are compared, for which there is some tension. As an application, the matrix elements are utilized to compute pion decay rates in a magnetic field.

## I. INTRODUCTION

The impact of magnetic fields on strongly interacting matter is important both theoretically and phenomenologically [1–3]. Magnetic fields alter the phase diagram of QCD. A prime example is magnetic catalysis, which enhances chiral symmetry breaking as characterized by the chiral condensate [4–6]. Additionally, they alter the nature of the confinement-deconfinement transition, which at weak magnetic fields is a crossover. For large magnetic fields, QCD becomes an anisotropic pure gauge theory that is known to possess a first-order deconfinement transition [7]. Magnetic fields also modify the phase diagram of QCD at finite isospin and baryon densities through the formation of magnetic vortices and chiral soliton lattices [8–13]. There is a wide array of studies exploring the magnetic field axis of the QCD phase diagram and various order parameters [14–32].

Phenomenologically, magnetic fields play an important role in astrophysical scenarios and at high-energy colliders. Magnetars support large surface magnetic fields  $\sim 10^{10}$  T, and even larger fields are expected in the interior of these neutron stars [33]. Magnetic fields of comparable sizes are possible in the cosmological electroweak phase transition from a quark-gluon soup to the confined hadronic phase following the Big Bang [34, 35]. In addition, off-central collisions of heavy ions at RHIC and the LHC produce considerably larger magnetic fields of size  $\sim 10^{16}$  T [36–40].

Chiral perturbation theory [41, 42] is an effective theory that allows for the study of low-energy QCD in a model-independent way, including the impact of magnetic fields of size  $eB \sim m_\pi^2$ , where  $m_\pi$  is the pion mass. As referenced above, it has been used to predict magnetic catalysis and the phase diagram of finite density QCD. Further work has addressed the impact of magnetic fields on pions and other hadrons, thermodynamic quantities, and finite-volume effects relevant for lattice QCD calculations [43–54]. In this work, we focus on the systematic computation of the left-handed vector current in chiral

perturbation theory. These contributions are interesting from the perspective of low-energy theorems in a magnetic field, while the main application of the result is to leptonic weak decays of mesons.

In a strong magnetic field, the charged pion becomes less stable due to an increase in its energy from Landau quantization.<sup>1</sup> Understanding pion stability may be important for magnetar physics, for example, through its influence on the high-energy neutrino spectrum produced from photo-meson processes [55]. Weak decay of mesons was the subject of a pioneering lattice QCD calculation [56]. A complete model-independent parametrization of the amplitudes entering the weak-decay matrix elements in a magnetic field was given in Refs. [57, 58]. Additional work on the subject has employed models, for which an incomplete list would be [59–67]. Here, our focus is exclusively on results that are consequences of low-energy QCD. There is an important distinction to be made between model insensitivity and model independence. While chiral perturbation theory restricts us to  $eB \sim m_\pi^2$ , the behavior in this regime provides stringent tests of both hadronic models and lattice QCD computations.

Our presentation has the following organization. Chiral perturbation theory in a magnetic field is reviewed in Sec. II. The left-handed vector current is obtained at next-to-leading order in the chiral expansion. As detailed in Appendix A, an additional tree-level contribution is obtained at next-to-next-to-leading order. The resulting vector and axial-vector currents are discussed along with low-energy theorems. A few comparisons are made with the pioneering lattice QCD calculation of Ref. [56], and with the Nambu–Jona-Lasinio model study carried out in Ref. [66]. As an application, the pion current matrix elements are then employed in Sec. III to calculate pion decay rates in a uniform magnetic field. For the neutral pion, we investigate its electromagnetic decay. While a new anomaly-mediated decay mechanism exists, the two-photon decay mode remains dominant. For the charged

\* adhika1@stolaf.edu

† btiburzi@ccny.cuny.edu

<sup>1</sup> Due to its magnetic moment, the ground-state energy of the outgoing lepton is almost independent of the magnetic field due to a near zero mode.

pion, its weak leptonic decay rate is explicitly shown to respect the residual  $SO(1,1) \times SO(2)$  Lorentz covariance. The neutrino angular asymmetry is used to explore the differential decay rate of longitudinally boosted pions. A final section, Sec. IV, provides a summary of the main results, and concludes with a few avenues for further investigation.

## II. CHIRAL LAGRANGIAN IN A MAGNETIC FIELD

To compute the weak decay rate of pions, we obtain the effective left-handed vector current of chiral perturbation theory. We use the two-flavor chiral Lagrangian [41] in the presence of an external magnetic field, which shares similarities with chiral perturbation theory with the inclusion of virtual photons [68]. Properties of the derived vector and axial-vector currents, as well as low-energy theorems, are then detailed.

### A. Leading Order

At leading order in the chiral expansion, the Lagrangian density is

$$\mathcal{L}_2 = \frac{F^2}{4} \langle \mathcal{D}^\mu U^\dagger \mathcal{D}_\mu U + U^\dagger \chi + \chi^\dagger U \rangle, \quad (1)$$

where angled brackets denote isospin traces and pions are embedded in the coset field  $U$  through  $U = \exp(i\phi \cdot \boldsymbol{\tau}/F)$ , with  $\tau^a$  as the isospin matrices. The canonically normalized pion fields are  $\pi^\pm = \frac{1}{\sqrt{2}}(\phi^1 \mp i\phi^2)$  and  $\pi^0 = \phi^3$ , which we will often abbreviate as  $\pi^Q$ , for  $Q = \pm 1$  and 0. The parameter  $F$  is the chiral-limit value of the pion-decay constant in vanishing magnetic field. External scalar  $s$  and pseudoscalar  $p$  sources are contained in the spurion field  $\chi = 2B_0(s + ip)$ , where the parameter  $B_0$  is related to the chiral-limit value of the chiral condensate  $\langle \bar{\psi}\psi \rangle_0 = -2B_0F^2$ . With the scalar source set equal to the quark mass  $m_q$  for vanishing pseudoscalar source, we obtain the Gell-Mann–Oakes–Renner relation  $m^2F^2 = -\langle \bar{\psi}\psi \rangle_0 m_q$ , where  $m$  is the tree-level pion mass. The vector source fields appear in Eq. (1) through the action of the gauge covariant derivative

$$\mathcal{D}^\mu U = \partial^\mu U + iUL^\mu - iR^\mu U, \quad (2)$$

where  $L^\mu$  is a left-handed vector field, and  $R^\mu$  is a right-handed vector field.

The left-handed current is obtained from differentiation with respect to the left-handed source field, which we decompose into isoscalar and isovector terms  $L^\mu = \frac{1}{2}\langle L^\mu \rangle \mathbb{1} + \sum_{a=1}^3 L^{\mu a} \tau^a$ . The isovector left-handed current in a background electromagnetic field is then

$$J_L^{\mu a} = \left. \frac{\partial \mathcal{L}}{\partial L_\mu^a} \right|_{L_\mu = R_\mu = -eQA_\mu}, \quad (3)$$

where  $e > 0$  is the magnitude of the electron's charge, and

$$Q = \frac{1}{6} \mathbb{1} + \frac{1}{2} \tau^3, \quad (4)$$

is the light quark charge matrix. The vector potential of the electromagnetic field is denoted by  $A_\mu$ , and we implement the magnetic field  $\mathbf{B} = B \hat{\mathbf{z}}$  using the asymmetric gauge  $A_\mu(x) = (0, -By, 0, 0)$ , and choose  $B > 0$ . With the magnetic field included in Eq. (1), the power counting is

$$p^2 \sim m_\pi^2 \sim eB \ll \Lambda_\chi, \quad (5)$$

where  $p$  is a good component of momentum and  $\Lambda_\chi = 4\pi F_\pi = 1.16 \text{ GeV}$  is the chiral symmetry breaking scale. While the magnetic field must be perturbatively small in the chiral expansion, this power counting accommodates fields that are large in physical terms, because  $eB/m_\pi^2 \sim 1$ .

The leading-order (LO) isovector left-handed current obtained from Eq. (1) is simply

$$\left( J_L^{\mu Q} \right)_{\text{LO}} = F D^\mu \pi^Q, \quad (6)$$

where  $J_L^{\mu Q}$  is shorthand for  $\frac{1}{\sqrt{2}}(J_L^{\mu 1} \pm iJ_L^{\mu 2})$  for  $Q = \pm 1$ , and  $J_L^{\mu 3}$  for  $Q = 0$ . The electromagnetic gauge covariant derivative of the pion field is specified by

$$D^\mu \pi^Q = (\partial^\mu + iQeA^\mu) \pi^Q. \quad (7)$$

As  $\mathcal{L}_2$  has even intrinsic parity, the LO contribution to the left-handed current is entirely axial vector in nature. For neutral pions, there is no effect from an electromagnetic field at LO; whereas, for charged pions, the effect is due to minimal coupling with the electromagnetic field.

### B. Next-To-Leading Order

At next-to-leading order (NLO) in the chiral expansion, there are several effects to account for. Expanding Eq. (1) to NLO generates one-loop diagrams that modify the effective action. Additionally, there are terms required from the NLO chiral Lagrangian  $\mathcal{L}_4$ . These include counter-terms necessary to renormalize the one-loop diagrams, but there are also finite contributions. The NLO effects are categorized below, with results given for both neutral and charged pions.

#### 1. Mass Renormalization

The four-pion terms obtained by expanding Eq. (1) to NLO generate tadpole diagrams that result in wavefunction and mass renormalization. There is also the mass counter-term  $l_3$  from the NLO chiral Lagrangian, which

cancels the ultraviolet divergence contained in the one-loop pion mass. As this counter-term is independent of the magnetic field, the renormalized magnetic mass is identical to that obtained from a simple zero-field subtraction. For the neutral pion, one obtains [44]

$$m_{\pi^0}^2(B) = m_\pi^2 \left[ 1 + \frac{eB}{\Lambda_\chi^2} \mathcal{F} \left( \frac{m_\pi^2}{eB} \right) \right], \quad (8)$$

where the function  $\mathcal{F}(z)$  arises from the charged-pion tadpole, and is given by

$$\mathcal{F}(z) = 2 \log \Gamma \left( \frac{1+z}{2} \right) + z \left( 1 - \log \frac{z}{2} \right) - \log 2\pi, \quad (9)$$

with  $\mathcal{F}(z) = -\frac{1}{6}z^{-1} + \mathcal{O}(z^{-3})$  for  $z \gg 1$ . The physical pion mass  $m_\pi$  and physical decay constant  $F_\pi$  appear in Eq. (8) up to corrections that are of next-to-next-to-leading order (NNLO).

For the charged pion, the one-loop contribution to its mass arises only from a neutral pion tadpole, after wavefunction renormalization is accounted for. This contribution is thus independent of the magnetic field to NNLO. There are, however, counter-terms that depend on external fields contained in the NLO chiral Lagrangian [41]

$$\begin{aligned} \mathcal{L}_4 \supset & l_5 \langle U^\dagger \hat{R}^{\mu\nu} U \hat{L}_{\mu\nu} \rangle \\ & + l_6 \frac{i}{2} \langle \mathcal{D}^\mu U^\dagger \mathcal{D}^\nu U \hat{L}_{\mu\nu} + \mathcal{D}^\mu U \mathcal{D}^\nu U^\dagger \hat{R}_{\mu\nu} \rangle, \end{aligned} \quad (10)$$

where the left- and right-handed field-strength tensor are defined by

$$\begin{aligned} L^{\mu\nu} &= \partial^\mu L^\nu - \partial^\nu L^\mu - i[L^\mu, L^\nu], \\ R^{\mu\nu} &= \partial^\mu R^\nu - \partial^\nu R^\mu - i[R^\mu, R^\nu]. \end{aligned} \quad (11)$$

The hats are employed to denote trace-subtracted quantities, so that for any matrix  $O$ , we have

$$\hat{O} = O - \frac{1}{2} \langle O \rangle \mathbb{1}. \quad (12)$$

The terms from  $\mathcal{L}_4$  contribute to the magnetic mass-squared of the charged pion<sup>2</sup>

$$m_{\pi^\pm}^2(B) = m_\pi^2 \left[ 1 + \bar{l} \frac{eB}{m_\pi^2} \frac{eB}{\Lambda_\chi^2} \right], \quad (13)$$

and encompasses its magnetic polarizability. We use the abbreviation

$$\bar{l} \equiv \frac{1}{3} (\bar{l}_6 - \bar{l}_5) = 1.0 \pm 0.1, \quad (14)$$

for the linear combination of renormalized low-energy constants. This combination is renormalization scale and scheme independent (the chiral logarithm cancels in the difference), and the value quoted is obtained from an NNLO analysis of rare pion decays [69].

## 2. Left-Handed Current Renormalization

In expanding Eq. (1) to NLO, there are three-pion terms<sup>3</sup> accompanied by one left-handed vector source  $L^\mu$ . These terms generate one-loop corrections to the left-handed current. Taken with the wavefunction renormalization, the divergence in these tadpole diagrams is canceled by the  $l_4$  counter-term from  $\mathcal{L}_4$ , which is independent of the magnetic field. Accordingly, the renormalized one-loop result in a magnetic field is identical to that obtained from a zero-field subtraction. The result is a renormalization of the leading-order current Eq. (6), where  $F$  is replaced by [44]

$$F_{\pi^Q}(B) = F_\pi \left[ 1 - \left( 1 - \frac{|Q|}{2} \right) \frac{eB}{\Lambda_\chi^2} \mathcal{F} \left( \frac{m_\pi^2}{eB} \right) \right], \quad (15)$$

where the tadpole function appears in Eq. (9).

The external-field dependent terms appearing in  $\mathcal{L}_4$  that are written in Eq. (10) also contribute to the left-handed current at NLO. Performing an integration by parts at the level of the action, we subsequently obtain from Eq. (3) a NLO contribution

$$\left( J_L^{\mu Q} \right)_{\text{NLO}} = -\bar{l} F_\pi \frac{iQ e F^{\mu\nu}}{\Lambda_\chi^2} D_\nu \pi^Q, \quad (16)$$

where  $\bar{l}$  is the linear combination of low-energy constants given in Eq. (14). This contribution to the left-handed current has axial-vector quantum numbers; and, it vanishes for the neutral pion due to charge conjugation.

The final contribution to the left-handed current at NLO arises from the chiral anomaly [70, 71]. The Wess-Zumino-Witten (WZW) Lagrangian [72, 73] has been constructed directly in two-flavor chiral perturbation theory in Ref. [74]. Retaining only the terms relevant for the left-handed current, we have

$$\begin{aligned} \mathcal{L}_4^{\text{WZW}} \supset & \frac{N_c}{64\pi^2} \varepsilon^{\mu\nu\alpha\beta} \left\langle i \left( U^\dagger \partial_\mu U \hat{L}_\nu - U \partial_\mu U^\dagger \hat{R}_\nu \right) \right. \\ & \left. + U^\dagger [\hat{R}_\mu, U] \hat{L}_\nu \right\rangle \langle L_{\alpha\beta} + R_{\alpha\beta} \rangle, \end{aligned} \quad (17)$$

with the convention that  $\varepsilon^{0123} = +1$ . Note that because a pure SU(2) theory has no anomalies, this Lagrangian density vanishes without the inclusion of isoscalar vector sources. Such a source is provided by an external electromagnetic field through the isoscalar contribution to the charge matrix.

<sup>2</sup> As is made clear in Eq. (49) below, the magnetic mass of the charged pion is defined to be the contribution to its energy that is independent of the Landau level quantum number.

<sup>3</sup> There are also two-pion terms with one left-handed source, but these do not contribute to pion decay. The origin of such terms is explained by writing  $L^\mu = V^\mu - \mathcal{A}^\mu$ , where  $V^\mu$  is a vector source and  $\mathcal{A}^\mu$  is an axial-vector source. From  $\mathcal{L}_2$ , which has even intrinsic parity, the terms with  $V^\mu$  have an even number of pions, while those with  $\mathcal{A}^\mu$  have an odd number of pions.

Appealing to Eq. (3), we obtain the final NLO contribution to the left-handed current using the WZW Lagrangian

$$\left(J_L^{\mu Q}\right)_{\text{WZW}} = -\frac{e\tilde{F}^{\mu\nu}}{8\pi^2 F_\pi} D_\nu \pi^Q, \quad (18)$$

where the dual electromagnetic field-strength tensor is  $\tilde{F}^{\mu\nu} = \frac{1}{2}\varepsilon^{\mu\nu\alpha\beta} F_{\alpha\beta}$ . This contribution to the current has vector quantum numbers because  $\mathcal{L}_4^{\text{WZW}}$  has odd intrinsic parity. Despite the necessary gauge non-invariance of the WZW Lagrangian, the anomalous contribution to the left-handed current appropriately maintains electromagnetic gauge covariance.

### C. Currents and Low-Energy Theorems

In a uniform magnetic field, general parameterizations of the vector and axial-vector current matrix elements of pions were given in Ref. [57]. To facilitate comparison with the NLO results obtained in chiral perturbation theory, we write analogous parameterizations in terms of the vector current operator

$$J_V^{\mu Q} = -e F_{\pi^Q}^{(V)} \tilde{F}^{\mu\nu} D_\nu \pi^Q \quad (19)$$

and the axial-vector current operator

$$J_A^{\mu Q} = -\left[ F_{\pi^Q}^{(A1)} D^\mu - iQe F_{\pi^Q}^{(A2)} F^{\mu\nu} D_\nu + e^2 F_{\pi^Q}^{(A3)} F^{\mu\nu} F_{\nu\alpha} D^\alpha \right] \pi^Q. \quad (20)$$

The amplitudes  $F^{(V)}$  and  $F^{(Aj)}$ , for  $j = 1-3$ , are generally required for pion weak decay in a uniform magnetic field, with only  $F^{(A1)}$  remaining in the zero-field limit. Note that the charge label appearing on  $F_{\pi^Q}^{(A2)}$  is superfluous. As written, it is identical for the charged pions, and necessarily drops out of the axial-vector current for neutral pions. These are consequences of charge conjugation.

Using the chiral perturbation theory calculation Eq. (18), we have the vector amplitudes

$$F_{\pi^\pm}^{(V)} = F_{\pi^0}^{(V)} = \frac{1}{8\pi^2 F_\pi} \left[ 1 + \mathcal{O}\left(\frac{eB}{\Lambda_\chi^2}\right) \right], \quad (21)$$

where these results are exactly fixed by the chiral anomaly up to NNLO corrections, the size of which has been indicated. Note that these corrections could equally well be typified as  $m_\pi^2/\Lambda_\chi^2$ , because we assume  $eB/m_\pi^2 \sim 1$ . The anomaly as the origin of the vector transition amplitude of a pion in a magnetic field was noted in Ref. [66]. Lattice QCD calculations of the vector-current matrix element of the pion in a background magnetic field therefore enable extraction of the

chiral anomaly.<sup>4</sup> The lattice QCD results for  $F_{\pi^\pm}^{(V)}$  approach a constant value in the limit of small magnetic fields [56]<sup>5</sup>

$$\frac{F_{\pi^\pm}^{(V)}(B=0)}{F_\pi} = \begin{cases} 1.2(3) \text{ GeV}^{-2} & \text{Wilson quarks} \\ 0.8(2) \text{ GeV}^{-2} & \text{Staggered quarks} \\ 1.49(3) \text{ GeV}^{-2} & \text{Anomaly, Eq. (16)} \end{cases}, \quad (22)$$

where the uncertainty in the theory prediction from the chiral anomaly is an estimate of pion-mass corrections at NNLO. The lattice data with quenched Wilson quarks are obtained with a larger-than-physical pion mass  $m_\pi \approx 415 \text{ GeV}$ , while the staggered data are obtained at the physical quark masses. The two lattice QCD results are consistent with each other. The prediction from the chiral anomaly is independent of the quark masses and of dynamical quarks, for which the agreement between fermion discretizations might be expected. Relative pion mass corrections to the Wilson results are expected to be roughly  $m_\pi^2/\Lambda_\chi^2 \sim 13\%$ , and the quenched Wilson lattice QCD result is thus completely consistent with the anomaly. Taken by itself, however, there is  $\sim 3.5\sigma$  tension between the fully dynamical staggered lattice QCD result at the physical pion mass and the value required by the chiral anomaly.

Returning to Eq. (20) to address the axial-vector amplitudes, the first is simply given by  $F_{\pi^Q}^{(A1)} = F_{\pi^Q}(B)$ , where the latter appears in Eq. (15). There are lattice QCD results for this amplitude [56], however, the axial-vector data appear to be described by linear  $eB$  dependence, for which a negative slope is found near  $eB = 0$ . By contrast, the chiral perturbation theory prediction from Eq. (15) requires strikingly different behavior

$$F_{\pi^\pm}(B) = F_\pi \left[ 1 + \frac{(eB)^2}{12m_\pi^2\Lambda_\chi^2} + \dots \right], \quad (23)$$

in the small-field limit  $eB/m_\pi^2 \ll 1$ . Even for magnetic fields satisfying  $eB \sim m_\pi^2$ , chiral perturbation theory requires  $F_{\pi^\pm}(B)/F_\pi > 1$ . Further data at smaller values of the external field strength would be required to establish that lattice QCD respects this model-independent behavior.

<sup>4</sup> In Ref. [56], the existence of the vector transition amplitude was interpreted in terms of  $\rho$ - $\pi$  mixing in a magnetic field [75]. While the chiral anomaly thus provides the mechanism for such mixing, obtaining a prediction for the mixing angle requires knowledge of the model-dependent coupling  $g_{\gamma\rho\pi}$  that appears in the Lagrangian density  $\mathcal{L} = \frac{1}{3}e g_{\gamma\rho\pi} \tilde{F}^{\mu\nu} \partial_\mu \rho_\nu \cdot \phi$ . In the phenomenologically successful vector-dominance model, this coupling vanishes in the chiral limit, see, for example, Ref. [76].

<sup>5</sup> Using their notation and conventions for the matrix element, the chiral anomaly leads to the prediction  $f'_\pi(0) = (4\pi^2 f_\pi)^{-1}$ . With the relation  $f_\pi = \sqrt{2} F_\pi$ , moreover, we see that  $f'_\pi(0)/f_\pi = F_{\pi^\pm}^{(V)}(0)/F_\pi$ .

For the two remaining axial-vector amplitudes in Eq. (20), chiral perturbation theory requires

$$F_{\pi^\pm}^{(A2)} = \frac{\bar{l}}{16\pi^2 F_\pi} \left[ 1 + \mathcal{O} \left( \frac{eB}{\Lambda_\chi^2} \right) \right], \quad (24)$$

$$F_{\pi^0}^{(A3)} = -\frac{c_{\pi^0}}{F_\pi^3} \left[ 1 + \mathcal{O} \left( \frac{eB}{\Lambda_\chi^2} \right) \right]. \quad (25)$$

Neither of these axial-vector amplitudes have been calculated with lattice QCD, for which the former is predicted from chiral perturbation theory with an uncertainty of 10%. The latter, however, vanishes at NLO, which is easily established from power counting.<sup>6</sup> The non-vanishing contribution obtained for the  $F_{\pi^0}^{(A3)}$  amplitude thus arises at NNLO, and requires operators contained in the  $\mathcal{L}_6$  chiral Lagrangian [77]. The calculation leading to Eq. (25) is described in Appendix A. There are no determinations of the required low-energy constants appearing in the  $c_{\pi^0}$  parameter, although there are resonance saturation estimates for some of the contributing terms [78].

With the currents Eqs. (19) and (20) derived in the effective theory, we can investigate conservation laws and additional low-energy theorems. The vector current of the neutral pion in an external field is conserved, which is easily demonstrated by taking the divergence

$$\partial_\mu J_V^{\mu 3} = 0, \quad (26)$$

and using the Maxwell equation  $\partial_\mu \tilde{F}^{\mu\nu} = 0$ . For the charged pion, the currents are necessarily only gauge covariant, for which it is natural to consider the gauge covariant derivative of the currents. Using the vector current of the charged pion from Eq. (19), we obtain the covariant divergence of the vector current

$$D_\mu J_V^{\mu\pm} = \pm 2ie^2 F_{\pi^0}^{(V)} \mathbf{E} \cdot \mathbf{B} \pi^\pm. \quad (27)$$

Hence, the vector current of charged pions is covariantly conserved in a uniform magnetic field.

Explicit chiral symmetry breaking is seen from the derivatives of the axial-vector currents. Taking the divergence of the neutral pion's axial-vector current Eq. (20), we obtain

$$\partial_\mu J_A^{\mu 0} = F_{\pi^0}(B) m_{\pi^0}^2(B) \pi^0, \quad (28)$$

for an on-shell  $\pi^0$ . Here, we have dropped the contribution from the term with  $F_{\pi^0}^{(A3)}$ , as this amplitude is zero at NLO. Non-zero quark masses lead to explicit chiral symmetry breaking, which manifests in the non-vanishing divergence. The divergence of the axial-vector current does vanish in the chiral limit, because  $m_{\pi^0}^2(B) \rightarrow 0$  for fixed magnetic field from Eq. (8). On the other hand,

the divergence of the axial-vector–pseudoscalar correlation function contains a pole

$$\int d^4x e^{ix \cdot p} \langle 0 | \partial_\mu J_A^{\mu 0}(x) \pi^0(0) | 0 \rangle = \frac{iF_{\pi^0}(B) p^2}{p^2 - m_{\pi^0}^2(B) + i\varepsilon}. \quad (29)$$

This divergence does not vanish when one takes the chiral limit before putting the pion on-shell, and the corresponding chiral symmetry is spontaneously broken. The neutral pion remains a pseudo-Goldstone boson in a magnetic field, and a straightforward generalization of the Gell-Mann–Oakes–Renner relation is satisfied. This can be confirmed explicitly to NLO by taking the ratio of the relation in a magnetic field to that in zero field

$$\frac{F_{\pi^0}^2(B) m_{\pi^0}^2(B)}{F_\pi^2 m_\pi^2} = \frac{\langle \bar{\psi}\psi \rangle_B}{\langle \bar{\psi}\psi \rangle_0} = 1 - \frac{eB}{\Lambda_\chi^2} \mathcal{J} \left( \frac{m_\pi^2}{eB} \right), \quad (30)$$

where the chiral condensate ratio on the right-hand side was first determined using chiral perturbation theory in Ref. [6].

For charged pions, the situation is different. The gauge covariant derivative of the current leads to

$$D_\mu J_A^{\mu\pm} = - \left[ F_{\pi^\pm}^{(A1)} D_\mu D^\mu + \frac{e^2}{2} F_{\pi^\pm}^{(A2)} F_{\mu\nu} F^{\mu\nu} \right] \pi^\pm, \quad (31)$$

where we have made use of the uniformity of the external field, and dropped the contribution from  $F_{\pi^\pm}^{(A3)}$  as it vanishes to NLO. In the case of charged pions, we can still appeal to the Green's function

$$\left[ D_\mu D^\mu + m_{\pi^\pm}^2(B) \right] G_\pm(x, 0) = -i\delta^{(4)}(x). \quad (32)$$

Notice that the Green's function is determined at NLO from the renormalized action, in which the charged pion mass has been replaced by the magnetic mass. After accounting for the wavefunction renormalization, the gauge covariant derivatives are not renormalized.

The un-amputated, coordinate-space correlation function between the current's divergence and the charged pion can be written in term of the Green's function. We find

$$\begin{aligned} \langle 0 | D_\mu J_A^{\mu\pm}(x) \pi^\pm(0) | 0 \rangle \\ = \left[ F_{\pi^\pm}^{(A1)} m_{\pi^\pm}^2(B) - F_{\pi^\pm}^{(A2)} (eB)^2 \right] G_\pm(x, 0), \end{aligned} \quad (33)$$

provided  $x_\mu \neq 0$ . This expression can be simplified further using the NLO quantities determined in Eqs. (13), (15), and (24). We find the simple result

$$\langle 0 | D_\mu J_A^{\mu\pm}(x) \pi^\pm(0) | 0 \rangle = F_{\pi^\pm}(B) m_\pi^2 G_\pm(x, 0), \quad (34)$$

up to NNLO corrections. At the level of the charged pion Green's function, the covariant divergence of the axial-vector current vanishes in the chiral limit. This result, however, is intermediate to those obtained for the neutral pion in Eqs. (28) and (29). The quark mass appears as

<sup>6</sup> This was pointed out in Ref. [44], where the decomposition of the axial-vector current Eq. (20) essentially already appears.

the source of explicit chiral symmetry breaking, however, spontaneous symmetry breaking cannot be exhibited for charged pions. While the Green's function maintains poles encompassing the Landau levels, the corresponding energies do not vanish in the chiral limit. Near a pole, the correlation function in Eq. (34) consequently vanishes in the chiral limit. In a magnetic field, the charged pion is technically no longer a pseudo-Goldstone boson.<sup>7</sup>

Despite this observation, explicit chiral symmetry breaking in the presence of a magnetic field  $eB \ll \Lambda_\chi^2$  still leads to a generalization of the Gell-Mann–Oakes–Renner relation. The simplicity of Eq. (34) is ultimately a reflection of the underlying QCD relation

$$D_\mu \left[ \bar{\psi}(x) \gamma^\mu \gamma^5 \tau^\pm \psi(x) \right] = (m_u + m_d) \bar{\psi}(x) i \gamma^5 \tau^\pm \psi(x), \quad (35)$$

in a magnetic field, where  $D_\mu$  is the electromagnetic gauge covariant derivative and  $\psi(x) = \begin{pmatrix} u(x) \\ d(x) \end{pmatrix}$  is the isodoublet of light quark fields. The isovector pseudoscalar current appearing in Eq. (35) can be obtained in the effective theory from differentiation with respect to the corresponding source

$$J_P^a = \frac{\partial \mathcal{L}}{\partial p^a}. \quad (36)$$

Using Eq. (1) in a background magnetic field (as well as the requisite field-independent counter-term from  $\mathcal{L}_4$ ), we find the charged pion pseudoscalar current at NLO can be written in the form

$$J_P^\pm = -\frac{\langle \bar{\psi} \psi \rangle_B}{F_{\pi^\pm}(B)} \pi^\pm \left[ 1 + \mathcal{O} \left( \frac{eB}{\Lambda_\chi^2} \right) \right]. \quad (37)$$

Upon taking the matrix element of Eq. (35) with a charged-pion field and amputating the Green's function, we arrive at the relation

$$F_{\pi^\pm}(B) m_\pi^2 = -(m_u + m_d) \frac{\langle \bar{\psi} \psi \rangle_B}{F_{\pi^\pm}(B)}, \quad (38)$$

which can be rearranged to form the ratio

$$\frac{F_{\pi^\pm}^2(B) m_\pi^2}{F_\pi^2 m_\pi^2} = \frac{\langle \bar{\psi} \psi \rangle_B}{\langle \bar{\psi} \psi \rangle_0}, \quad (39)$$

where we have retained the  $m_\pi^2$  in the numerator and denominator to better indicate how this is a generalization of the Gell-Mann–Oakes–Renner relation. Using Eq. (15) for  $F_{\pi^\pm}(B)$  and the right-hand side of Eq. (30) for the

<sup>7</sup> In the chiral limit, the two-flavor QCD action in a magnetic field maintains only the diagonal  $U(1)_L \times U(1)_R$  subgroup of the  $SU(2)_L \times SU(2)_R$  chiral symmetry group that exists in vanishing magnetic field. The neutral pion emerges as the pseudo-Goldstone boson associated with the spontaneous breaking of  $U(1)_L \times U(1)_R \rightarrow U(1)_V$ .

chiral condensate ratio, the charged pion relation above is indeed satisfied at NLO.

Additionally, due to the numerical value of the low-energy constant  $\bar{l}$  in Eq. (14), one has the approximate relation

$$F_{\pi^\pm}^{(V)} - 2 F_{\pi^\pm}^{(A2)} \approx 0 + \mathcal{O} \left( \frac{eB}{\Lambda_\chi^3} \right), \quad (40)$$

which is satisfied at the 10% level given the uncertainty in the extraction of  $\bar{l}$  from data. This relation appears to be a numerical coincidence, rather than a low-energy theorem. Nonetheless, it should be contrasted with the chiral-limit behavior of the results obtained from the Nambu–Jona-Lasinio model study in Ref. [66, Eq. (93)], which instead lead to the relation<sup>8</sup>

$$F_{\pi^\pm}^{(V)} - F_{\pi^\pm}^{(A2)} = 0 + \mathcal{O} \left( \frac{eB}{\Lambda_\chi^3} \right). \quad (41)$$

This relation is at odds with chiral perturbation theory.

Finally, there is a relation between the  $F^{(A3)}$  amplitude and the anisotropy in the pion dispersion relation.<sup>9</sup> This was discussed in Ref. [66], but only for the neutral pion. In that work, the relation is found due to a Goldberger-Treiman relation for the pion coupling to a constituent quark-antiquark pair in the chiral limit. Independent of model assumptions, the relation emerges from the structure of operators contained in the  $\mathcal{L}_6$  chiral Lagrangian. Utilizing the result from Appendix A, the single-pion effective action at NNLO has the general form

$$\begin{aligned} \mathcal{L} = & \frac{1}{2} \pi^0 \left[ -\partial^\mu \partial_\mu - \frac{(eB)^2}{F_\pi^4} c_{\pi^0} \partial_\perp^\mu \partial_{\perp\mu} - m_{\pi^0}^2(B) \right] \pi^0 \\ & + \pi^+ \left[ -D^\mu D_\mu - \frac{(eB)^2}{F_\pi^4} c_{\pi^\pm} D_\perp^\mu D_{\perp\mu} - m_{\pi^\pm}^2(B) \right] \pi^-, \end{aligned} \quad (42)$$

after wave-function renormalization has been taken into account. The general form of this effective action can be argued based on symmetry principles. In a uniform magnetic field, the Lorentz symmetry group is reduced to an  $SO(1,1) \times SO(2)$  subgroup [79]. The effect in chiral perturbation theory can be quantified through the factor

$$Z_\perp^Q = 1 + \frac{(eB)^2}{F_\pi^4} c_{\pi^Q}, \quad (43)$$

<sup>8</sup> Note that we have changed their notation to ours. For small magnetic fields, their  $f_{\pi^-}^{(V)}$  and  $f_{\pi^-}^{(A2)}$  amplitudes each contain an overall factor of  $eB$ , while their  $f_{\pi^-}^{(A3)}$  amplitude contains an overall factor of  $(eB)^2$ . Removing an overall  $eB$ , the latter amplitude accordingly does not appear in Eq. (41), having been absorbed into the correction term.

<sup>9</sup> While the dispersion relation for charged pions is already anisotropic, the form of the charged-pion effective Lagrangian in Eq. (42) represents an additional anisotropy beyond the spectrum of  $D^\mu D_\mu$  in a fixed background field.

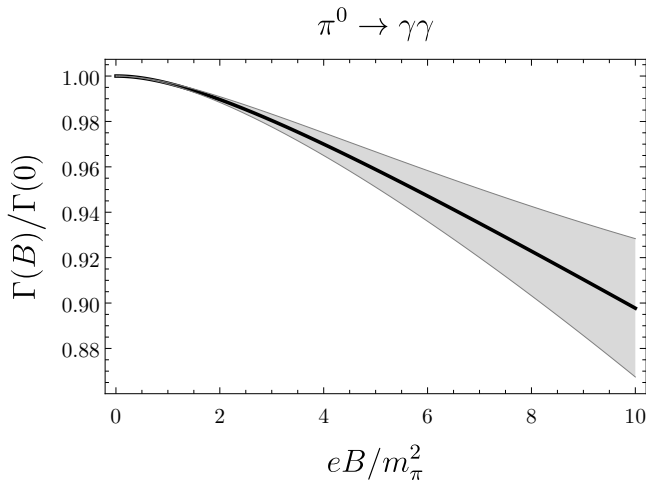


FIG. 1. Neutral pion decay in a magnetic field. The ratio of the decay rate Eq. (46) for the anomalous process  $\pi^0 \rightarrow \gamma\gamma$  in a magnetic field to that in zero magnetic field is plotted as a function of the magnetic field strength. The uncertainty band is generated by varying the relative NNLO correction between  $\pm(eB)^2/\Lambda_\chi^4$ .

which represents the residual renormalization factor for the transverse directions. The deviation from unity must be quite small for  $eB \sim m_\pi^2$ ; but, in principle, can be deduced from the pion dispersion relation. Nonetheless, the fact that the same parameter  $c_{\pi Q}$  enters the amplitude  $F^{(A3)}$  leads to the NNLO relation

$$(eB)^2 F_{\pi Q}^{(A3)} = (1 - Z_\perp^Q) F_{\pi Q}^{(A1)}, \quad (44)$$

for both neutral and charged pions. The result for the neutral pion agrees with that found in Ref. [66], while the charged pion relation was not investigated in their model study.

### III. PION DECAYS

#### A. Neutral Pion Decay

While the weak decay rate of the neutral pion in a magnetic field can be computed from results above, electromagnetic processes mediated by the chiral anomaly are considerably more important. Decay through the anomalous process  $\pi^0 \rightarrow \gamma\gamma$  is the dominant decay mode. The pertinent term obtained from expanding the two-flavor WZW Lagrangian Eq. (17) is well known

$$\mathcal{L}_4^{\text{WZW}} \supset -\frac{\alpha}{\pi} \frac{\pi^0}{F_\pi} \mathbf{E} \cdot \mathbf{B}. \quad (45)$$

Accounting for all NLO terms in the chiral expansion, the two-photon decay rate in a magnetic field becomes

$$\Gamma_{\pi^0 \rightarrow \gamma\gamma}(B) = \frac{\alpha^2 m_{\pi^0}^3(B)}{4\pi\Lambda_\chi^2}, \quad (46)$$

and depends on the magnetic field through the neutral pion's magnetic mass. As shown in Fig. 1, the decay rate decreases with increasing magnetic field, which is entirely driven by the decrease in available energy.

In vanishing magnetic field, the anomaly-mediated process  $\pi^0 \rightarrow e^+e^-$  is considerably suppressed compared to two-photon decay, in part due to two additional electromagnetic vertices (for a recent review and update, see Ref. [80]). The term in Eq. (45), however, leads to a new mechanism for this decay in an external magnetic field. With the electric field providing a virtual photon, the vertex mediates the anomalous process

$$\pi^0 \xrightarrow{B} \gamma^* \rightarrow e^+e^-. \quad (47)$$

While the coupling between the  $\pi^0$  and a virtual photon increases linearly with increasing magnetic field, the allowed phase space for an electron-positron pair (each in their lowest Landau level) vanishes beyond the value  $eB_{\text{max}} = \frac{1}{2}m_{\pi^0}^2(B) - m_e^2$ . For moderately sized fields satisfying  $B < B_{\text{max}}$ , there is a substantial increase in the rate for the process  $\pi^0 \rightarrow e^+e^-$  over the  $B = 0$  mechanism; however, the decay  $\pi^0 \rightarrow \gamma\gamma$  certainly remains the overwhelmingly dominant mode.

#### B. Charged Pion Decay

To compute the weak decay rate of the charged pion, we first specify the kinematics. For simplicity, we describe the calculation for the positively charged pion  $\pi^+ \rightarrow \ell^+ \nu_\ell$ . We have verified that the negatively charged pion decay rate is identical, which provides a non-trivial check of the final result. With the gauge choice employed throughout, the good components of momentum for a charged particle are denoted by

$$\tilde{P}^\mu = (E, \tilde{\mathbf{P}}), \quad \text{where} \quad \tilde{\mathbf{P}} = (P_x, 0, P_z). \quad (48)$$

While  $\tilde{P}^\mu$  is certainly not a four-vector, the  $SO(1,1)$  subgroup of longitudinal Lorentz transformations is maintained. Note that the interpretation of the  $P_x$  quantum number as momentum is gauge dependent [81].

In the  $N$ -th Landau level, the charged pion energy is given by

$$E_{N,P_z} = \sqrt{m_{\pi^\pm}^2(B) + (2N+1)eB + P_z^2}, \quad (49)$$

where the magnetic mass of the charged pion  $m_{\pi^\pm}(B)$  appears in Eq. (13). The spectrum's  $P_x$ -independence reflects the infinite degeneracy of Landau levels. The decay rate itself is demonstrably independent of  $P_x$  [57], which provides circumstantial evidence for gauge invariance. Direct evidence has been obtained by verifying the total decay rate is identical using the symmetric gauge [58].

The spectrum of an anti-lepton of mass  $m_\ell$  in the final state can be written as

$$E_{n,p_z} = \sqrt{m_\ell^2 + 2neB + p_z^2}, \quad (50)$$

where each energy eigenstate has a two-fold infinite degeneracy, with degeneracy labels  $s = \pm\frac{1}{2}$  and  $p_x$ . The exceptions are states with  $n = 0$ , for which only the  $z$ -component of spin  $s = +\frac{1}{2}$  is possible. We have used  $n$  as one of the quantum numbers; it is related to the usual Landau level quantum number  $n_L$  through  $n = n_L - s + \frac{1}{2}$ . The neutrino final state is labeled by its  $z$ -component of spin  $s'$  and four-momentum  $q^\mu$ .

Treating all momentum quantum numbers of the decay implicitly, the coordinate-space amplitude for charged pion leptonic decay is

$$\mathcal{M}_n^{s's}(x) = G_F V_{\text{ud}} \left[ \bar{u}_q^{s'}(x) \gamma_\mu (1 - \gamma^5) V_n^s \tilde{p}(x) \right] \times \langle 0 | J_L^{\mu+}(x) | \pi_{N, \tilde{\mathbf{P}}}^+ \rangle, \quad (51)$$

where  $G_F$  is the Fermi coupling constant, and  $V_{\text{ud}}$  is the light-quark weak mixing matrix element. The coordinate-space spinor  $\bar{u}_q^{s'}(x)$  is that for the neutrino, which is just the Fourier phase multiplied by the conventionally defined on-shell momentum spinor  $\bar{u}_q^{s'}(x) = e^{iq \cdot x} u^{s'}(q)$ . The coordinate-space spinor for an on-shell anti-lepton is  $V_n^s \tilde{p}(x)$ , and satisfies a generalization of the standard normalization condition

$$\int d^3x \bar{V}_n^s \tilde{p}(x) V_{n'}^{s'} \tilde{p}'(x) = -2m_\ell \delta^{ss'} \delta^{nn'} (2\pi)^2 \delta^{(2)}(\tilde{\mathbf{p}} - \tilde{\mathbf{p}}'), \quad (52)$$

when integrated over all space. Given the left-handed current at NLO in the effective theory, one readily computes its single-pion-to-vacuum matrix element appearing in the amplitude Eq. (51).

Appealing to conservation of the good components of momentum, we define a reduced amplitude through the relation

$$\int d^3\tilde{x} \mathcal{M}_n^{s's}(x) \equiv (2\pi)^3 \delta^{(2)}(\tilde{\mathbf{P}} - \tilde{\mathbf{p}} - \tilde{\mathbf{q}}) \times \delta(E_{N, P_z} - E_{n, p_z} - E_q) \mathcal{M}_{n, \text{red}}^{s's}(y), \quad (53)$$

where the integration is over all coordinates canonically conjugate to the good components of momentum. We use shorthand for the evaluation at  $x^\mu|_{\tilde{x}^\mu=0}$  as simply  $x = y$ . The coordinate dependence of the reduced amplitude reflects the Fourier transform of the displaced coordinate overlap between the pion Landau level and that of the anti-lepton.

With these specifications, the total decay rate for the process  $\pi^+ \rightarrow \ell^+ \nu_\ell$  is given by

$$\Gamma_\ell(B) = \frac{1}{2E_{N, P_z}} \sum_n \int \frac{d^3q d^2\tilde{p}}{2E_q 2E_{n, p_z} (2\pi)^5} \langle |\mathcal{M}_n|^2 \rangle \times (2\pi)^3 \delta^{(2)}(\tilde{\mathbf{P}} - \tilde{\mathbf{p}} - \tilde{\mathbf{q}}) \delta(E_{N, P_z} - E_{n, p_z} - E_q), \quad (54)$$

where the modulus squared amplitude summed over final state spins is defined as

$$\langle |\mathcal{M}_n|^2 \rangle = \sum_{s's} \left| \int dy \mathcal{M}_{n, \text{red}}^{s's}(y) \right|^2. \quad (55)$$

Although only  $n$  is labeled,  $\langle |\mathcal{M}_n|^2 \rangle$  is additionally a function of the initial-state quantum numbers  $N$  and  $P_z$ , as well as the final-state quantum numbers  $\tilde{\mathbf{p}}$  and  $\mathbf{q}$ . The momentum  $P_x$  produces an overall phase in  $\mathcal{M}_{n, \text{red}}^{s's}(y)$  that cancels in the modulus squared.

In the total decay rate, the pre-factor  $E_{N, P_z}^{-1}$  is not invariant under longitudinal Lorentz transformations; instead, a boosted pion with  $\beta = P_z/E_{N, P_z}$  experiences time dilation governed by the factor

$$\gamma = \sqrt{1 - \beta^2} = \frac{E_{N, 0}}{E_{N, P_z}}. \quad (56)$$

Accordingly, the remaining factors must be invariant under longitudinal Lorentz transformations to ensure covariance of the decay rate. As the phase space and energy-momentum conserving delta functions in Eq. (54) satisfy such invariance, it must be that  $\langle |\mathcal{M}_n|^2 \rangle$  is invariant under the  $SO(1, 1) \times SO(2)$  subgroup of Lorentz transformations, which we verify below.

While the full formula for  $\langle |\mathcal{M}_n|^2 \rangle$  is rather lengthy, there is a reduction in the number of terms if we specify that the initial-state pion is in the lowest Landau level  $N = 0$ . When the magnetic field is suitably large, there will be a large gap between the lowest Landau level and the excited levels. In such cases, we can assume that all excited states have radiated down to the lowest Landau level before the weak decay. The large gap provides a suitably large phase space for the radiative decay, which will then occur on shorter time scales than the weak decay.

Restricting to  $N = 0$ , there are different contributions for the lepton energy levels  $n = 0$  and  $n \neq 0$ . Such differences arise due to the exclusion of the  $s = -\frac{1}{2}$  spin state for  $n = 0$ . As the amplitude  $F^{(A3)}$  vanishes at NLO, all contributions can be written in terms of three combinations of the remaining amplitudes

$$\begin{aligned} \mathcal{A} &= F_{\pi^\pm}^{(A1)} + eB F_{\pi^\pm}^{(V)}, \\ \mathcal{B} &= F_{\pi^\pm}^{(A1)} - eB F_{\pi^\pm}^{(V)}, \\ \mathcal{C} &= F_{\pi^\pm}^{(A1)} + eB F_{\pi^\pm}^{(A2)}. \end{aligned} \quad (57)$$

In terms of these combinations, we have<sup>10</sup>



$$\langle |\mathcal{M}_n|^2 \rangle = 8G_F^2 V_{ud}^2 \exp(-\zeta) \left\{ \frac{\zeta^n}{n!} \left[ \frac{\mathcal{A}^2}{2} P^- q^+ P^- p^+ + eB \mathcal{C} \mathcal{E}^2 q^- p^+ \frac{(n-\zeta)^2}{\zeta} + 2eB \mathcal{A} \mathcal{C} P^- p^+ (n-\zeta) \right] + (1-\delta_{n0}) \frac{\zeta^{n-1}}{(n-1)!} \left[ \frac{\mathcal{B}^2}{2} P^+ q^- P^+ p^- - 2eB \mathcal{A} \mathcal{B} P^+ P^- \zeta - 2eB \mathcal{B} \mathcal{C} P^+ q^- (n-\zeta) \right] \right\}, \quad (58)$$

where we employ the abbreviation

$$\zeta = \frac{\mathbf{q}_\perp^2}{2eB}, \quad (59)$$

with  $\mathbf{q}_\perp$  as the neutrino momentum transverse to the magnetic field. The dependence on  $\zeta$  ensures that the decay rate is  $SO(2)$  invariant. For any (1+1)-dimensional Lorentz vector with components  $a^0$  and  $a^3$ , the corresponding light-front components employed above are defined by

$$a^\pm = a^0 \pm a^3. \quad (60)$$

Products of the form  $a^+ b^-$  and  $a^- b^+$  are invariant under longitudinal Lorentz boosts. Accordingly, the modulus squared amplitude in Eq. (58) is manifestly invariant under  $SO(1,1)$ . This confirms that time dilation is the only effect on the total decay rate of a longitudinally boosted pion compared to a pion at rest  $P_z = 0$ .

Enforcing the decay kinematics through the delta-functions in Eq. (54) produces a constraint on the allowed lepton energy levels, namely  $n \leq n_{\max}$ , where

$$n_{\max} = \frac{m_{\pi^\pm}^2(B) - m_\ell^2}{2eB} + \frac{1}{2}, \quad (61)$$

which, for convenience, is not defined to be an integer. Conservation of the good components of momentum fixes the magnitude of the neutrino's momentum to be

$$|\mathbf{q}_0| = \frac{E_{0,P_z} - P_z x}{1 - x^2} - \frac{\sqrt{(E_{0,P_z} - P_z x)^2 - 2eB(n_{\max} - n)(1 - x^2)}}{1 - x^2}, \quad (62)$$

where  $x = \cos\theta$ , and  $\theta$  is the angle of the neutrino's momentum with the respect to the magnetic field. The differential decay rate for an initial-state pion in its lowest Landau level can thus be written in the form

$$\frac{d\Gamma_\ell(B)}{dx} = \frac{1}{16\pi E_{0,P_z}} \sum_{n=0}^{[n_{\max}]} \frac{|\mathbf{q}_0| \langle |\mathcal{M}_n|^2 \rangle}{E_{0,P_z} - P_z x - (1 - x^2) |\mathbf{q}_0|}, \quad (63)$$

<sup>10</sup> Aside from an overall factor of  $(2\pi)^2$ , the amplitude squared agrees with the general formula given in Ref. [57, Eq. (45)], when specialized to the case of an initial-state pion in the lowest Landau level  $N = 0$ . The difference in normalization is accounted for by a compensating factor of  $(2\pi)^{-2}$  in the decay rate Eq. (54).

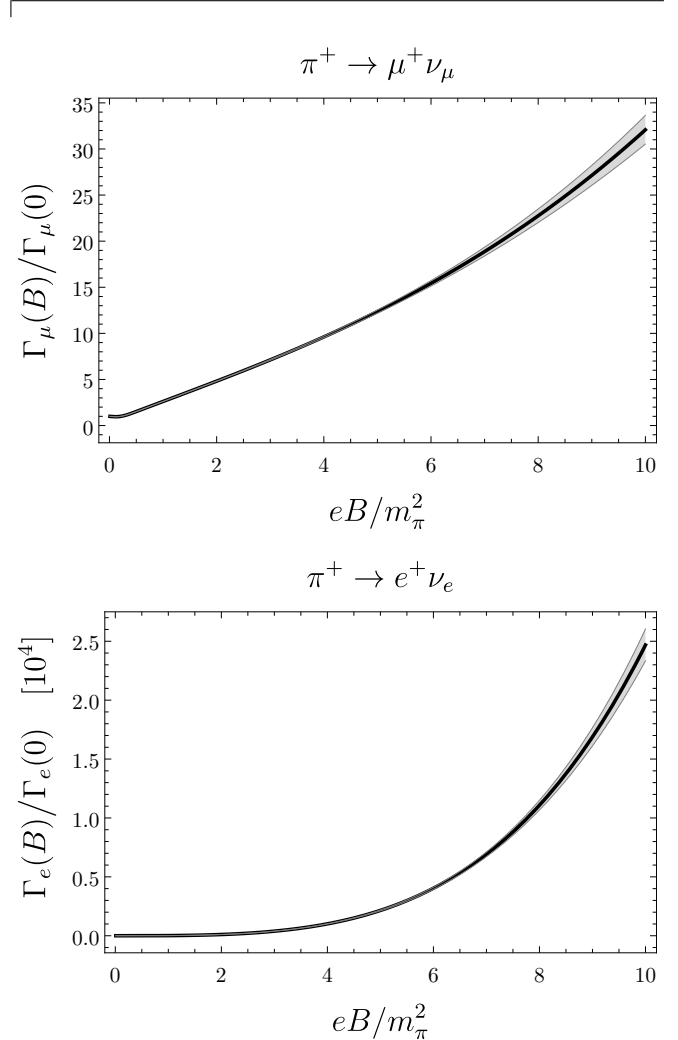


FIG. 2. Charged pion decay in a magnetic field. The ratio of the decay rate Eq. (54) in a magnetic field to that in zero magnetic field Eq. (64) is plotted as a function of the magnetic field strength for muonic and electronic decay modes. The uncertainty band is generated by varying the relative NNLO correction between  $\pm 2(eB)^2/\Lambda_\chi^4$ , as well as varying the low-energy constant  $\bar{l}$  within its uncertainties.

with the total decay rate given as the integral over all possible angles  $\Gamma_\ell(B) = \int_{-1}^{+1} \frac{d\Gamma_\ell(B)}{dx} dx$ .

The charged pion decay rate for muonic and electronic decay modes is plotted as a function of the magnetic field

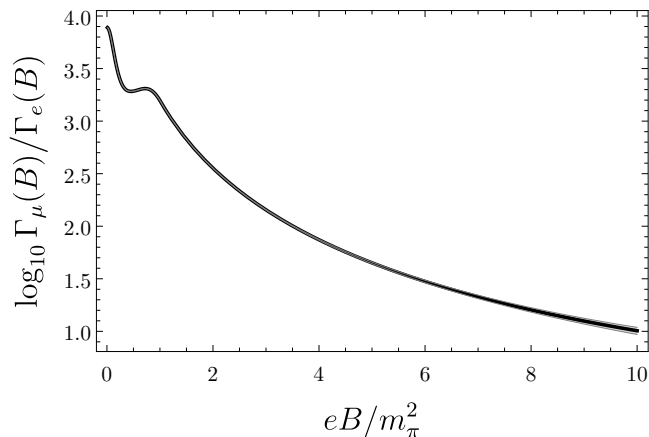


FIG. 3. Comparison of the charged pion’s muonic and electronic decay modes. The logarithm of the ratio of partial widths (muonic to electronic) is plotted as a function of the magnetic field. While we include an uncertainty band generated in the same manner as Fig. 2, it can barely be discerned from the width of the curve plotted.

strength in Fig. 2. Each decay rate is plotted as a ratio to the corresponding rate in vanishing magnetic field

$$\Gamma_\ell(0) = \frac{G_F^2 V_{ud}^2 F_\pi^2}{4\pi} m_\pi m_\ell^2 \left(1 - \frac{m_\ell^2}{m_\pi^2}\right)^2. \quad (64)$$

This rate, however, does not directly arise from the zero-field limit of Eq. (54), due to the restriction of the initial-state pion to its lowest Landau level.<sup>11</sup> Both partial widths have increased compared to their corresponding zero-field widths. In the case of the electronic decay mode, the width is substantially greater, because the magnetic field allows the electron to overcome helicity suppression. The electronic decay mode, however, becomes comparable to the muonic one as the magnetic field strength increases. In zero magnetic field, the ratio of partial widths is  $\Gamma_\mu(0)/\Gamma_e(0) \approx 10^4$ . In Fig. 3, the magnetic field dependence of this ratio is plotted as a function of  $eB/m_\pi^2$ . While the muonic decay mode remains more probable than the electronic decay mode, it is no longer overwhelmingly preferred. The ratio approaches 10.1(5) for the largest magnetic field shown. The wiggle in the ratio for small values of the magnetic field is primarily due to the muonic decay mode, which does not increase monotonically in this region.

While the total decay rate only depends on  $P_z$  through the time-dilation factor, the differential decay rate has a more complicated dependence on the pion’s longitudinal momentum. To investigate this dependence, we form the

<sup>11</sup> It has been shown, however, that the zero-field result properly emerges after adjusting the overall normalization from that of a discrete Landau level to that of a continuum zero-momentum state [57].

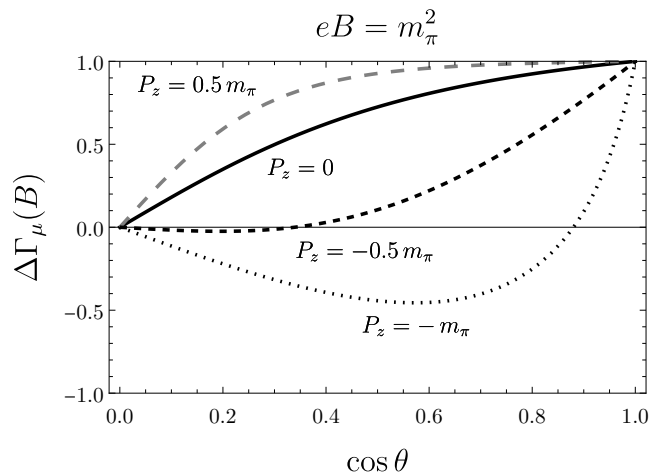


FIG. 4. Angular asymmetry in the differential decay width. Using a fixed value of the magnetic field, the asymmetry Eq. (65) of the decay  $\pi^+ \rightarrow \mu^+ \nu_\mu$  is plotted as a function of  $x = \cos \theta$ , for a few values of the pion’s longitudinal momentum  $P_z$ .

angular asymmetry in the differential decay rate

$$\Delta\Gamma_\ell(B) = \frac{\frac{d\Gamma_\ell(B)}{dx}\Big|_x - \frac{d\Gamma_\ell(B)}{dx}\Big|_{-x}}{\frac{d\Gamma_\ell(B)}{dx}\Big|_x + \frac{d\Gamma_\ell(B)}{dx}\Big|_{-x}}. \quad (65)$$

The component of the neutrino’s momentum in the direction of the magnetic field can be positive or negative. When it is equally likely to be positive or negative, the asymmetry vanishes  $\Delta\Gamma_\ell(B) = 0$ . The angular asymmetry is shown in Fig. 4 for the muonic decay mode at a fixed value of the external field. Already for a pion at rest  $P_z = 0$ , the neutrino emerges with a  $z$ -component of momentum preferentially in the direction of the magnetic field. Of course, this bias for the magnetic field direction only increases when the pion is also moving in the same direction. When the pion is moving in the direction opposite of the magnetic field with a suitably large momentum, however, there can be more neutrinos emerging with their  $z$ -component of momentum anti-aligned with the field. This can happen for a range of  $\cos \theta$ , away from the value  $\cos \theta = 1$ .

#### IV. SUMMARY AND CONCLUSIONS

The hadronic left-handed vector current in an external magnetic field is studied systematically using chiral perturbation theory. This analysis provides model-independent constraints on pion matrix elements that arise due to the pattern of explicit and spontaneous symmetry breaking in low-energy QCD. These constraints constitute low-energy theorems that must be satisfied by lattice QCD calculations, and additionally provide stringent tests for models of hadronic physics (for example, the relation Eq. (40) is not satisfied by the results of the

model study in Ref. [66]). While the applicability of chiral perturbation theory limits one to perturbatively small fields  $eB \ll \Lambda_\chi^2$ , the results serve to anchor the behavior of observables in the regime  $eB \sim m_\pi^2$ .

As the chiral anomaly is the source of the vector-pseudoscalar coupling in an external magnetic field, the  $F^{(V)}$  amplitude provides a relatively straightforward means to directly measure the chiral anomaly in lattice QCD. Beyond the pioneering work in Ref. [56], further calculations are needed to address the tension Eq. (22) between the result for staggered quarks at the physical quark masses and the chiral anomaly. Additional calculations are warranted for the  $F^{(A1)}$  amplitude in a magnetic field. The small-field behavior observed empirically from lattice QCD data is at odds with that obtained from chiral perturbation theory Eq. (23). The Gell-Mann–Oakes–Renner relations in a magnetic field Eqs. (30) and (39), furthermore, allow one to relate magnetic catalysis to the increase in  $F^{(A1)}$  amplitudes in a magnetic field.

The remaining axial-vector amplitudes,  $F^{(A2)}$  and  $F^{(A3)}$ , provide an opportunity to extract low-energy constants of chiral perturbation theory from lattice QCD. For both of these amplitudes, the same low-energy constants enter the pion spectrum, which can thereby be utilized for a consistency check on the calculations, or provide additional data to constrain these numerically small contributions. For  $F^{(A2)}$ , the underlying physics is that of the charged pion magnetic polarizability; whereas, for  $F^{(A3)}$ , the underlying physics is the magnetic field induced anisotropy in the pion dispersion relation.

With the model-independent results from chiral perturbation theory, the dominant decays of neutral and charged pions are computed in the  $eB \sim m_\pi^2$  regime. For the neutral pion, the electromagnetic decay rate via the anomalous process  $\pi^0 \rightarrow \gamma\gamma$  appears in Fig. 1, where a modest decrease with increasing magnetic field is shown. Although other decay mechanisms become available in an external magnetic field, the zero-field decay mode remains the dominant one. For the charged pion, we explicitly verify the  $SO(1,1) \times SO(2)$  covariance of its weak decay rate. Time-dilation is thereby the only effect on the total decay rate of a longitudinally moving pion. The electronic decay mode is greatly enhanced, consistent with the lack of helicity suppression in a magnetic field [56, 67]. In the regime where our results apply, the muonic decay mode is still dominant, but only by at most a factor of  $\sim 10$ . For the differential decay rate, we explore the longitudinal momentum dependence through the angular asymmetry Eq. (65). Rather large momentum antiparallel to the field (for example,  $P_z = -m_\pi$ ) is needed to overcome the bias for the magnetic field direction in the emerging neutrinos.

The analysis can be generalized to three-flavor chiral perturbation theory, as well as carried out at non-zero temperature. Higher-order effects would be interesting to ascertain, even if only their signs. The behavior of the magnetic mass of the neutral pion, for example, is intriguing, for which the natural question is whether the

NNLO contribution also decreases with increasing magnetic field. Additionally the qualitative behavior of the NNLO contribution to the axial-vector amplitude  $F^{(A1)}$  may shed light on the strikingly different behavior seen in lattice QCD data. Finally, a higher-order calculation of the chiral anomaly in an external magnetic field would be beneficial to address the low-energy QCD prediction for the  $F^{(V)}$  amplitude, and its subsequent extraction from future lattice QCD data.

## ACKNOWLEDGEMENTS

P.A. is supported in part by the U.S. Department of Energy, Office of Science, Office of Nuclear Physics and Quantum Horizons Program under Award Number DE-SC0024385. P.A. acknowledges the hospitality of The City College of New York, the Graduate Center of the City University of New York, and that of the Kavli Institute for Theoretical Physics, Santa Barbara, through which the research was supported in part by the U.S. National Science Foundation under Grant No. NSF PHY-1748958.

### Appendix A: Tree-Level Contribution at Next-To-Next-To-Leading Order

The first non-vanishing contribution to the  $F^{(A3)}$  amplitude in Eq. (20) occurs at NNLO in chiral perturbation theory from two-loop and one-loop diagrams, as well as from tree-level operators. The full NNLO calculation is beyond the scope of this work; however, the structure of the answer, aside from chiral logarithms, can be deduced solely from the tree-level contribution. To this end, we require terms from the two-flavor  $\mathcal{L}_6$  Lagrangian [77]

$$\begin{aligned} Y_{31} &= \langle \hat{f}_{+\mu\nu} \hat{f}_+^{\mu\alpha} u^\nu u_\alpha \rangle, \\ Y_{32} &= \langle \hat{f}_{+\mu\nu} \hat{f}_+^{\mu\alpha} u_\alpha u^\nu \rangle, \\ Y_{33} &= \left\langle \hat{f}_{+\mu\nu} \left( u_\alpha \hat{f}_+^{\mu\alpha} u^\nu + u^\nu \hat{f}_+^{\mu\alpha} u_\alpha \right) \right\rangle. \end{aligned} \quad (\text{A1})$$

These operators have been written using the traceless vielbein field

$$u_\mu = i \left[ u^\dagger \left( \partial_\mu - i \hat{R}_\mu \right) u - u \left( \partial_\mu - i \hat{L}_\mu \right) u^\dagger \right], \quad (\text{A2})$$

and the chirally covariant field-strength tensor  $\hat{f}_+^{\mu\nu}$ , which is defined by

$$\hat{f}_+^{\mu\nu} = u \hat{L}^{\mu\nu} u^\dagger + u^\dagger \hat{R}^{\mu\nu} u. \quad (\text{A3})$$

The compensator field  $u$  is determined from the coset field  $U$  appearing in Eq. (1) through the relation  $u^2 = U$ . The Lagrangian is formed from sums of the  $Y_j$  operators weighted by  $F^{-2} c_j$ , so that the corresponding low-energy constants  $c_j$  are dimensionless.

The construction of the minimal operator basis in Ref. [77] makes explicit use of traceless left- and right-handed vector fields. For an electromagnetic field, there is no effect on  $u_\mu$  in Eq. (A2), because the isoscalar component of the gauge field decouples. Similarly, isoscalar gauge fields decouple from the terms of the  $\mathcal{L}_4$  Lagrangian density Eq. (10), aside from a pion-independent contact term. The same is not true for  $\mathcal{L}_6$ , and two additional operators with isoscalar gauge fields are needed. We take these operators to be

$$\begin{aligned}\tilde{Y}_{31} &= \langle L_{\mu\nu} + R_{\mu\nu} \rangle \langle L^{\mu\alpha} + R^{\mu\alpha} \rangle \langle u^\nu u_\alpha \rangle, \\ \tilde{Y}_{32} &= i \langle L_{\mu\nu} + R_{\mu\nu} \rangle \langle \hat{f}_+^{\mu\alpha} [u^\nu, u_\alpha] \rangle.\end{aligned}\quad (\text{A4})$$

Note that an operator similar to  $\tilde{Y}_{32}$  but with  $i [u^\nu, u_\alpha]$  replaced by  $\{u^\nu, u_\alpha\}$  identically vanishes. The isoscalar gauge field contributions to the Lagrangian require a sum over the  $\tilde{Y}_j$  operators weighted by  $F^{-2} \tilde{c}_j$ , where the corresponding low-energy constants  $\tilde{c}_j$  are dimensionless.

With the requisite terms of  $\mathcal{L}_6$  spelled out, we can obtain the isovector left-handed current in a background electromagnetic field using Eq. (3). This produces the contribution

$$\left( J_L^{\mu Q} \right)_{\text{NNLO}} = -c_{\pi Q} \frac{e^2}{F^3} F^{\mu\alpha} F_{\mu\beta} D^\beta \pi^Q, \quad (\text{A5})$$

from which the axial-vector amplitude  $F_{\pi Q}^{(A3)}$  reported in

Eq. (25) follows. The parameters  $c_{\pi Q}$  involve linear combinations of the low-energy constants

$$c_{\pi Q} = 4 \left[ c_{31} + c_{32} + 2(1-2|Q|)c_{33} + \frac{4}{9} \tilde{c}_{31} \right] + f_{\pi Q}(m_\pi), \quad (\text{A6})$$

for which the contribution from the  $\tilde{Y}_{32}$  operator drops out. The running of  $c_{33}$  obtained in Ref. [82], for example, points to the necessity of chiral logarithms from loop diagrams, which have been denoted by  $f_{\pi Q}(m_\pi)$ . Accordingly, the sum of these contributions renders the  $c_{\pi Q}$  renormalization scale independent.

An additional feature of the operators listed in Eqs. (A1) and (A4) is that they modify the pion dispersion relation in an anisotropic way. Expanding these terms of the NNLO chiral Lagrangian density in a uniform magnetic field, we have the two-pion terms

$$\mathcal{L}_6 \supset \frac{(eB)^2}{F^4} \left[ \frac{1}{2} c_{\pi^0} \partial_\perp^\mu \pi^0 \partial_{\perp\mu} \pi^0 + c_{\pi^\pm} D_\perp^\mu \pi^+ D_{\perp\mu} \pi^- \right], \quad (\text{A7})$$

where  $a_\perp^\mu = (0, a^1, a^2, 0)$  is used to denote the components of a four-vector that are transverse to the time and field directions. The parameters  $c_{\pi Q}$  are exactly the same linear combinations of renormalized low-energy constants and chiral logarithms appearing in Eq. (A6). As a result, the anisotropy in the dispersion relations of neutral and charged pions is related to the  $F^{(A3)}$  amplitude, which is exhibited in Eq. (44).

- 
- [1] D. E. Kharzeev, K. Landsteiner, A. Schmitt, and H.-U. Yee, Strongly interacting matter in magnetic fields, *Lect. Notes Phys.* **871**, 10.1007/978-3-642-37305-3 (2013), arXiv:1211.6245 [hep-ph].
- [2] J. O. Andersen, W. R. Naylor, and A. Tranberg, Phase diagram of QCD in a magnetic field: A review, *Rev. Mod. Phys.* **88**, 025001 (2016), arXiv:1411.7176 [hep-ph].
- [3] V. A. Miransky and I. A. Shovkovy, Quantum field theory in a magnetic field: From quantum chromodynamics to graphene and Dirac semimetals, *Phys. Rept.* **576**, 1 (2015), arXiv:1503.00732 [hep-ph].
- [4] I. A. Shushpanov and A. V. Smilga, Quark condensate in a magnetic field, *Phys. Lett. B* **402**, 351 (1997), arXiv:hep-ph/9703201.
- [5] N. O. Agasian and I. A. Shushpanov, The Quark and gluon condensates and low-energy QCD theorems in a magnetic field, *Phys. Lett. B* **472**, 143 (2000), arXiv:hep-ph/9911254.
- [6] T. D. Cohen, D. A. McGady, and E. S. Werbos, The Chiral condensate in a constant electromagnetic field, *Phys. Rev. C* **76**, 055201 (2007), arXiv:0706.3208 [hep-ph].
- [7] T. D. Cohen and N. Yamamoto, New critical point for QCD in a magnetic field, *Phys. Rev. D* **89**, 054029 (2014), arXiv:1310.2234 [hep-ph].
- [8] P. Adhikari, T. D. Cohen, and J. Sakowitz, Finite Isospin Chiral Perturbation Theory in a Magnetic Field, *Phys. Rev. C* **91**, 045202 (2015), arXiv:1501.02737 [nucl-th].
- [9] P. Adhikari, Magnetic Vortex Lattices in Finite Isospin Chiral Perturbation Theory, *Phys. Lett. B* **790**, 211 (2019), arXiv:1810.03663 [nucl-th].
- [10] P. Adhikari, E. Leeser, and J. Markowski, Phonon modes of magnetic vortex lattices in finite isospin chiral perturbation theory, *Mod. Phys. Lett. A* **38**, 2350078 (2023), arXiv:2205.13369 [hep-ph].
- [11] T. Brauner and N. Yamamoto, Chiral Soliton Lattice and Charged Pion Condensation in Strong Magnetic Fields, *Journal of High Energy Physics* **04**, 132 (2017), arXiv:1609.05213 [hep-ph].
- [12] T. Brauner, H. Kolešová, and N. Yamamoto, Chiral soliton lattice phase in warm QCD, *Phys. Lett. B* **823**, 136767 (2021), arXiv:2108.10044 [hep-ph].
- [13] G. W. Evans and A. Schmitt, Chiral anomaly induces superconducting baryon crystal, *Journal of High Energy Physics* **09**, 192 (2022), arXiv:2206.01227 [hep-th].
- [14] M. D'Elia, S. Mukherjee, and F. Sanfilippo, QCD Phase Transition in a Strong Magnetic Background, *Phys. Rev. D* **82**, 051501 (2010), arXiv:1005.5365 [hep-lat].
- [15] M. D'Elia and F. Negro, Chiral Properties of Strong Interactions in a Magnetic Background, *Phys. Rev. D* **83**, 114028 (2011), arXiv:1103.2080 [hep-lat].
- [16] G. S. Bali, F. Bruckmann, G. Endrodi, Z. Fodor, S. D. Katz, S. Krieg, A. Schafer, and K. K. Szabo, The QCD phase diagram for external magnetic fields, *Journal of High Energy Physics* **02**, 044 (2012), arXiv:1111.4956

- [hep-lat].
- [17] G. S. Bali, F. Bruckmann, G. Endrodi, Z. Fodor, S. D. Katz, and A. Schafer, QCD quark condensate in external magnetic fields, *Phys. Rev. D* **86**, 071502 (2012), arXiv:1206.4205 [hep-lat].
- [18] G. S. Bali, F. Bruckmann, M. Constantinou, M. Costa, G. Endrodi, S. D. Katz, H. Panagopoulos, and A. Schafer, Magnetic susceptibility of QCD at zero and at finite temperature from the lattice, *Phys. Rev. D* **86**, 094512 (2012), arXiv:1209.6015 [hep-lat].
- [19] G. S. Bali, F. Bruckmann, G. Endrodi, F. Gruber, and A. Schaefer, Magnetic field-induced gluonic (inverse) catalysis and pressure (an)isotropy in QCD, *Journal of High Energy Physics* **04**, 130 (2013), arXiv:1303.1328 [hep-lat].
- [20] F. Bruckmann, G. Endrodi, and T. G. Kovacs, Inverse magnetic catalysis and the Polyakov loop, *Journal of High Energy Physics* **04**, 112 (2013), arXiv:1303.3972 [hep-lat].
- [21] C. Bonati, M. D'Elia, M. Mariti, F. Negro, and F. Sanfilippo, Magnetic Susceptibility of Strongly Interacting Matter across the Deconfinement Transition, *Phys. Rev. Lett.* **111**, 182001 (2013), arXiv:1307.8063 [hep-lat].
- [22] C. Bonati, M. D'Elia, M. Mariti, F. Negro, and F. Sanfilippo, Magnetic susceptibility and equation of state of  $N_f = 2 + 1$  QCD with physical quark masses, *Phys. Rev. D* **89**, 054506 (2014), arXiv:1310.8656 [hep-lat].
- [23] G. S. Bali, F. Bruckmann, G. Endrodi, and A. Schafer, Paramagnetic squeezing of QCD matter, *Phys. Rev. Lett.* **112**, 042301 (2014), arXiv:1311.2559 [hep-lat].
- [24] V. G. Bornyakov, P. V. Buividovich, N. Cundy, O. A. Kochetkov, and A. Schäfer, Deconfinement transition in two-flavor lattice QCD with dynamical overlap fermions in an external magnetic field, *Phys. Rev. D* **90**, 034501 (2014), arXiv:1312.5628 [hep-lat].
- [25] G. S. Bali, F. Bruckmann, G. Endrödi, S. D. Katz, and A. Schäfer, The QCD equation of state in background magnetic fields, *Journal of High Energy Physics* **08**, 177 (2014), arXiv:1406.0269 [hep-lat].
- [26] G. Endrodi, Critical point in the QCD phase diagram for extremely strong background magnetic fields, *Journal of High Energy Physics* **07**, 173 (2015), arXiv:1504.08280 [hep-lat].
- [27] M. D'Elia, F. Manigrasso, F. Negro, and F. Sanfilippo, QCD phase diagram in a magnetic background for different values of the pion mass, *Phys. Rev. D* **98**, 054509 (2018), arXiv:1808.07008 [hep-lat].
- [28] G. S. Bali, G. Endrödi, and S. Piemonte, Magnetic susceptibility of QCD matter and its decomposition from the lattice, *Journal of High Energy Physics* **07**, 183 (2020), arXiv:2004.08778 [hep-lat].
- [29] H.-T. Ding, C. Schmidt, A. Tomiya, and X.-D. Wang, Chiral phase structure of three flavor QCD in a background magnetic field, *Phys. Rev. D* **102**, 054505 (2020), arXiv:2006.13422 [hep-lat].
- [30] H. T. Ding, S. T. Li, A. Tomiya, X. D. Wang, and Y. Zhang, Chiral properties of (2+1)-flavor QCD in strong magnetic fields at zero temperature, *Phys. Rev. D* **104**, 014505 (2021), arXiv:2008.00493 [hep-lat].
- [31] M. D'Elia, L. Maio, F. Sanfilippo, and A. Stanzione, Phase diagram of QCD in a magnetic background, *Phys. Rev. D* **105**, 034511 (2022), arXiv:2111.11237 [hep-lat].
- [32] H. T. Ding, S. T. Li, J. H. Liu, and X. D. Wang, Chiral condensates and screening masses of neutral pseudoscalar mesons in thermomagnetic QCD medium, *Phys. Rev. D* **105**, 034514 (2022), arXiv:2201.02349 [hep-lat].
- [33] A. K. Harding and D. Lai, Physics of Strongly Magnetized Neutron Stars, *Rept. Prog. Phys.* **69**, 2631 (2006), arXiv:astro-ph/0606674.
- [34] T. Vachaspati, Magnetic fields from cosmological phase transitions, *Phys. Lett. B* **265**, 258 (1991).
- [35] T. Vachaspati, Progress on cosmological magnetic fields, *Rept. Prog. Phys.* **84**, 074901 (2021), arXiv:2010.10525 [astro-ph.CO].
- [36] D. E. Kharzeev, L. D. McLerran, and H. J. Warringa, The Effects of topological charge change in heavy ion collisions: Event by event P and CP violation, *Nucl. Phys. A* **803**, 227 (2008), arXiv:0711.0950 [hep-ph].
- [37] V. Skokov, A. Y. Illarionov, and V. Toneev, Estimate of the magnetic field strength in heavy-ion collisions, *Int. J. Mod. Phys. A* **24**, 5925 (2009), arXiv:0907.1396 [nucl-th].
- [38] W.-T. Deng and X.-G. Huang, Event-by-event generation of electromagnetic fields in heavy-ion collisions, *Phys. Rev. C* **85**, 044907 (2012), arXiv:1201.5108 [nucl-th].
- [39] G. Inghirami, M. Mace, Y. Hirono, L. Del Zanna, D. E. Kharzeev, and M. Bleicher, Magnetic fields in heavy ion collisions: flow and charge transport, *Eur. Phys. J. C* **80**, 293 (2020), arXiv:1908.07605 [hep-ph].
- [40] M. I. Abdulhamid, B. E. Aboona, J. Adam, J. R. Adams, G. Agakishiev, I. Aggarwal, M. M. Aggarwal, Z. Ahammed, A. Aitbaev, *et al.* (STAR Collaboration), Observation of the electromagnetic field effect via charge-dependent directed flow in heavy-ion collisions at the relativistic heavy ion collider, *Phys. Rev. X* **14**, 011028 (2024).
- [41] J. Gasser and H. Leutwyler, Chiral Perturbation Theory to One Loop, *Annals Phys.* **158**, 142 (1984).
- [42] J. Gasser and H. Leutwyler, Chiral Perturbation Theory: Expansions in the Mass of the Strange Quark, *Nucl. Phys. B* **250**, 465 (1985).
- [43] E. S. Werbos, The Chiral condensate in a constant electromagnetic field at  $O(p^6)$ , *Phys. Rev. C* **77**, 065202 (2008), arXiv:0711.2635 [hep-ph].
- [44] B. C. Tiburzi, Hadrons in Strong Electric and Magnetic Fields, *Nucl. Phys. A* **814**, 74 (2008), arXiv:0808.3965 [hep-ph].
- [45] J. O. Andersen, Thermal pions in a magnetic background, *Phys. Rev. D* **86**, 025020 (2012), arXiv:1202.2051 [hep-ph].
- [46] J. O. Andersen, Chiral perturbation theory in a magnetic background - finite-temperature effects, *Journal of High Energy Physics* **10**, 005 (2012), arXiv:1205.6978 [hep-ph].
- [47] B. C. Tiburzi, Neutron in a Strong Magnetic Field: Finite Volume Effects, *Phys. Rev. D* **89**, 074019 (2014), arXiv:1403.0878 [hep-lat].
- [48] A. Deshmukh and B. C. Tiburzi, Octet Baryons in Large Magnetic Fields, *Phys. Rev. D* **97**, 014006 (2018), arXiv:1709.04997 [hep-ph].
- [49] C. P. Hofmann, Pion Pressure in a Magnetic Field, *Phys. Rev. D* **101**, 114031 (2020), arXiv:2004.01247 [hep-ph].
- [50] C. P. Hofmann, Chiral Perturbation Theory Analysis of the Quark Condensate in a Magnetic Field, *Phys. Rev. D* **102**, 094010 (2020), arXiv:2006.07717 [hep-ph].
- [51] C. P. Hofmann, Thermomagnetic properties of QCD, *Phys. Rev. D* **104**, 014025 (2021), arXiv:2012.06461 [hep-ph].
- [52] P. Adhikari, Topological susceptibility in a uniform magnetic field, *Phys. Lett. B* **825**, 136826 (2022),

- arXiv:2103.05048 [hep-ph].
- [53] P. Adhikari, QCD  $\theta$ -vacuum in a uniform magnetic field, Nucl. Phys. B **974**, 115627 (2022), arXiv:2111.06196 [hep-ph].
- [54] P. Adhikari and B. C. Tiburzi, QCD thermodynamics and neutral pion in a uniform magnetic field: Finite volume effects, Phys. Rev. D **107**, 094504 (2023), arXiv:2302.09179 [hep-lat].
- [55] B. Zhang, Z. G. Dai, and P. Meszaros, High-energy neutrinos from magnetars, Astrophys. J. **595**, 346 (2003), arXiv:astro-ph/0210382.
- [56] G. S. Bali, B. B. Brandt, G. Endrődi, and B. Gläbke, Weak decay of magnetized pions, Phys. Rev. Lett. **121**, 072001 (2018), arXiv:1805.10971 [hep-lat].
- [57] M. Coppola, D. Gomez Dumm, S. Noguera, and N. N. Scoccola, Pion-to-vacuum vector and axial vector amplitudes and weak decays of pions in a magnetic field, Phys. Rev. D **99**, 054031 (2019), arXiv:1810.08110 [hep-ph].
- [58] M. Coppola, D. Gomez Dumm, S. Noguera, and N. N. Scoccola, Weak decays of magnetized charged pions in the symmetric gauge, Phys. Rev. D **101**, 034003 (2020), arXiv:1910.10814 [hep-ph].
- [59] S. Fayazbakhsh, S. Sadeghian, and N. Sadooghi, Properties of neutral mesons in a hot and magnetized quark matter, Phys. Rev. D **86**, 085042 (2012), arXiv:1206.6051 [hep-ph].
- [60] S. Fayazbakhsh and N. Sadooghi, Weak decay constant of neutral pions in a hot and magnetized quark matter, Phys. Rev. D **88**, 065030 (2013), arXiv:1306.2098 [hep-ph].
- [61] K. Kamikado and T. Kanazawa, Chiral dynamics in a magnetic field from the functional renormalization group, Journal of High Energy Physics **03**, 009 (2014), arXiv:1312.3124 [hep-ph].
- [62] Y. A. Simonov, Pion decay constants in a strong magnetic field, Phys. Atom. Nucl. **79**, 455 (2016), arXiv:1503.06616 [hep-ph].
- [63] S. S. Avancini, R. L. S. Farias, M. Benghi Pinto, W. R. Tavares, and V. S. Timóteo,  $\pi_0$  pole mass calculation in a strong magnetic field and lattice constraints, Phys. Lett. B **767**, 247 (2017), arXiv:1606.05754 [hep-ph].
- [64] D. Gómez Dumm, M. F. Izzo Villafañe, and N. N. Scoccola, Neutral meson properties under an external magnetic field in nonlocal chiral quark models, Phys. Rev. D **97**, 034025 (2018), arXiv:1710.08950 [hep-ph].
- [65] M. A. Andreichikov and Y. A. Simonov, Chiral physics in the magnetic field with quark confinement contribution, Eur. Phys. J. C **78**, 902 (2018), arXiv:1805.11896 [hep-ph].
- [66] M. Coppola, D. Gomez Dumm, S. Noguera, and N. N. Scoccola, Neutral and charged pion properties under strong magnetic fields in the NJL model, Phys. Rev. D **100**, 054014 (2019), arXiv:1907.05840 [hep-ph].
- [67] M. Coppola, D. Gomez Dumm, S. Noguera, and N. N. Scoccola, Magnetic field driven enhancement of the weak decay width of charged pions, Journal of High Energy Physics **09**, 058 (2020), arXiv:1908.10765 [hep-ph].
- [68] R. Urech, Virtual Photons in Chiral Perturbation Theory, Nucl. Phys. B **433**, 234 (1995), arXiv:hep-ph/9405341.
- [69] J. Bijnens and G. Ecker, Mesonic Low-Energy Constants, Ann. Rev. Nucl. Part. Sci. **64**, 149 (2014), arXiv:1405.6488 [hep-ph].
- [70] S. L. Adler, Axial vector vertex in spinor electrodynamics, Phys. Rev. **177**, 2426 (1969).
- [71] J. S. Bell and R. Jackiw, A PCAC puzzle:  $\pi^0 \rightarrow \gamma\gamma$  in the  $\sigma$  model, Nuovo Cim. A **60**, 47 (1969).
- [72] J. Wess and B. Zumino, Consequences of anomalous Ward identities, Phys. Lett. B **37**, 95 (1971).
- [73] E. Witten, Global Aspects of Current Algebra, Nucl. Phys. B **223**, 422 (1983).
- [74] R. Kaiser, Anomalies and WZW Term of Two-Flavor QCD, Phys. Rev. D **63**, 076010 (2001), arXiv:hep-ph/0011377.
- [75] G. S. Bali, B. B. Brandt, G. Endrődi, and B. Gläbke, Meson masses in electromagnetic fields with Wilson fermions, Phys. Rev. D **97**, 034505 (2018), arXiv:1707.05600 [hep-lat].
- [76] M. Harada and K. Yamawaki, Hidden local symmetry at loop: A New perspective of composite gauge boson and chiral phase transition, Phys. Rept. **381**, 1 (2003), arXiv:hep-ph/0302103.
- [77] J. Bijnens, G. Colangelo, and G. Ecker, The Mesonic chiral Lagrangian of order  $p^6$ , Journal of High Energy Physics **02**, 020 (1999), arXiv:hep-ph/9902437.
- [78] V. Cirigliano, G. Ecker, M. Eidemuller, R. Kaiser, A. Pich, and J. Portoles, Towards a consistent estimate of the chiral low-energy constants, Nucl. Phys. B **753**, 139 (2006), arXiv:hep-ph/0603205.
- [79] V. A. Miransky and I. A. Shovkovy, Magnetic catalysis and anisotropic confinement in QCD, Phys. Rev. D **66**, 045006 (2002), arXiv:hep-ph/0205348.
- [80] T. Husek, The neutral-pion decay into electron-positron pair: A review and update, (2024), arXiv:2405.09650 [hep-ph].
- [81] T. Haugset, J. A. Ruud, and F. Ravndal, Gauge invariance of Landau levels, Physica Scripta **47**, 715 (1993).
- [82] J. Bijnens, G. Colangelo, and G. Ecker, Renormalization of chiral perturbation theory to order  $p^6$ , Annals Phys. **280**, 100 (2000), arXiv:hep-ph/9907333.